

# TECHNICAL PROGRESS REPORT

## Investigation of the Properties of Acid-Contaminated Sediment and its Effect on Contaminant Mobility

**Date Submitted:**

February 13, 2017

**Principal Investigator:**

Leonel E. Lagos, Ph.D., PMP®

**FIU Applied Research Center Collaborators:**

Yelena Katsenovich, Ph.D.  
Vasileios Anagnostopoulos, Ph.D.  
Awmna Rana, DOE Fellow

**SRNL Collaborator:**

Miles Denham, Ph.D.

**Prepared for:**

U.S. Department of Energy  
Office of Environmental Management  
Under Cooperative Agreement No. DE-EM0000598



### **DISCLAIMER**

This report was prepared as an account of work sponsored by an agency of the United States government. Neither the United States government nor any agency thereof, nor any of their employees, nor any of its contractors, subcontractors, nor their employees makes any warranty, express or implied, or assumes any legal liability or responsibility for the accuracy, completeness, or usefulness of any information, apparatus, product, or process disclosed, or represents that its use would not infringe upon privately owned rights. Reference herein to any specific commercial product, process, or service by trade name, trademark, manufacturer, or otherwise does not necessarily constitute or imply its endorsement, recommendation, or favoring by the United States government or any other agency thereof. The views and opinions of authors expressed herein do not necessarily state or reflect those of the United States government or any agency thereof.

## Table of Contents

1. Introduction .....	1
2. Objectives .....	1
3. Materials and Methods.....	2
3.1 Soil Samples and Working Solutions .....	2
3.2 Batch Experiments .....	2
3.3 Elemental Analysis.....	2
4. Results and Discussion .....	2
4.1 Preliminary Kinetic Results.....	2
4.2 Creation of Different Profiles of Acid-Treated Soil.....	8
5. Future Work .....	10
6. References.....	11

## List of Figures

Figure 1. Concentrations of Al (blue), Fe (red) and Si (green) released into the supernatant of batch experiments containing 4g of SRS F/H area soil (0.18<d<2 mm fraction) brought in contact with nitric acid solution of pH 2.5, as a function of time.....	3
Figure 2. Concentrations of Al (blue) and Si (green) released into the supernatant of batch experiments containing 4g of SRS F/H area soil (0.18<d<2 mm fraction) brought in contact with nitric acid solution of pH 2.5, as a function of time. Error bars represent the standard deviation of triplicate samples. ....	4
Figure 3. Concentrations of Fe released into the supernatant of batch experiments containing 4g of SRS F/H area soil (0.18<d<2 mm fraction) brought in contact with nitric acid solution of pH 2.5, as a function of time. Error bars represent the standard deviation of triplicate samples. ....	5
Figure 4. Speciation diagram of aqueous species and solid phases as a function of pH for Al, predicted by Hydra-Medusa Equilibrium Speciation Diagram. ....	7
Figure 5. Speciation diagram of aqueous species and solid phases as a function of pH for Si, predicted by Hydra-Medusa Equilibrium Speciation Diagram. ....	7
Figure 6. Concentration of Al (ppb) in the supernatant solution as a function of time. Error bars represent the standard deviation of triplicate samples. Red arrows are pointing to the time interval where the supernatant was replenished.....	8
Figure 7. Concentration of Fe (ppb) in the supernatant solution as a function of time. Error bars represent the standard deviation of triplicate samples. Red arrows are pointing to the time interval where the supernatant was replenished.....	9
Figure 8. Concentration of Si (ppb) in the supernatant solution as a function of time. Error bars represent the standard deviation of triplicate samples. Red arrows are pointing to the time interval where the supernatant was replenished.....	9
Figure 9. Concentration of Al and Si (ppb) in the supernatant solution as a function of time. Error bars represent the standard deviation of triplicate samples. Red arrows are pointing to the time interval where the supernatant was replenished.....	10

## List of Tables

Table 1. Concentration of Fe, Al and Si for Each SRS Fraction Followed by Relative Standard Deviation and Percentage Leached During the Preliminary Kinetic Experiment .....	5
Table 2. Major Aqueous and Saturated Species at pH 2.5, as Predicted by Visual Minteq .....	6

## 1. Introduction

The Savannah River Site (SRS) was established as one of the major sites for the production of materials related to the U.S. nuclear program during the early 1950s. An estimated 36 metric tons of plutonium were produced during the period 1953-1988. Since then, it has become a hazardous waste management facility responsible for nuclear storage and remediation of contaminated soil and groundwater from radionuclides. The groundwater at the F/H Area Seepage Basins Groundwater Operable Units at SRS was impacted by operations of the Hazardous Waste Management Facilities (HWMFs). Approximately 1.8 billion gallons (7.1 billion liters) and 1.6 billion gallons (6.0 billion liters) of low-level waste solutions have been received in the F and H areas respectively, originating from the processing of uranium slugs and irradiated fuel at the separation facilities. The effluents were acidic (wastewater contaminated with nitric acid) and low-activity waste solutions containing a wide variety of radionuclides and dissolved metals. Waste solutions were transported approximately 3,000 feet from each processing area through underground vitrified clay pipes to the basins. After entering the basin, the wastewater was allowed to evaporate and to seep into the underlying soil. The purpose of the basins was to take advantage of the interaction with the basin soils to minimize the migration of contaminants to exposure points. Though the seepage basins essentially functioned as designed, the acidic nature of the basin influent caused mobilization of metals and radionuclides resulting in groundwater contaminant plumes.

Currently, more than 235 monitoring wells at the site are sampled for a variety of chemical and radioactive parameters. Groundwater monitoring results have indicated the presence of elevated levels of metals, radionuclides and nitrates. Significant chemical differences exist between the groundwater from the two areas. The F Area groundwater contains higher concentrations of dissolved metals than that in the H Area. The constituents of concern (COCs) associated with the F Area HWMF groundwater plume are tritium ( $^3\text{H}$ ), uranium U-238, iodine I-129, strontium Sr-90, curium Cm-244, americium Am-241, technetium Tc-99, cadmium (Cd), and aluminum (Al). The COCs in the H Area are tritium, Sr-90, and mercury (Hg).

## 2. Objectives

The main objective of this study is to assess the impact of prolonged contact between soil and the acidic waste stream. More specifically, morphological and physico-chemical characteristics, such as specific surface area and pore distribution, may change due to extended contact between the soil and the acidic stream. Consequently, a change in specific surface area and pore distribution of the soil, as well as associated reaction products due to the mineral dissolution, may affect contaminant mobility, since these parameters are known to affect a substrate's ability to retain metals. Hence, different "acidified soil profiles" (soil that has come into contact with nitric acid for different time intervals) will be created, their physico-chemical properties will be evaluated and then ultimately used for sorption experiments. The results will be compared with the equivalent sorption results of background soil (SRS F/H Area not contaminated soil), as well as actual contaminated soil from the same area.

### **3. Materials and Methods**

#### **3.1 Soil Samples and Working Solutions**

Soil samples from the SRS F/H Area were sieved (USA Standard Testing Sieves, Fisher Scientific) and fractions of mean diameter  $0.18 < d < 2$  mm were stored temporarily in a desiccator, which contained anhydrous calcium sulfate (Drierite, Drierite Company Inc). The sieved fractions were used throughout the experimental process.

Deionized water (Barnstead NANOpure water purification system) was spiked with nitric acid ( $\text{HNO}_3$ ) until the final pH value was 2.5 (ThermoScientific pH electrode).

#### **3.2 Batch Experiments**

4 g of SRS soil, mean diameter  $0.18 < d < 2$  mm, were brought into contact with 130 ml of nitric acid, pH 2.5 in plastic vials. Every day (approximately 24h intervals) an aliquot was isolated from the supernatant, diluted 1:10 with 1% nitric acid, and stored at  $4^\circ \text{C}$  until analysis. All experiments were performed at room temperature ( $20^\circ \text{C}$ ).

#### **3.3 Elemental Analysis**

The concentrations of aluminum (Al), iron (Fe) and silica (Si) in the collected samples were analyzed by means of inductively coupled plasma - optical emission spectroscopy (ICP-OES 7300 Optima, Perkin Elmer). Al and Si can be traced to the soil's composition of quartz and kaolinite, while Fe can be traced to goethite. Future sorption experiments of the acid treated soil will involve uranium, and uranium analysis is going to be performed by means of Kinetic Phosphorescence Analysis (KPA).

### **4. Results and Discussion**

#### **4.1 Preliminary Kinetic Results**

The concentration of Al, Fe and Si in the supernatant as a function of time is presented in Figure 1. All experimental points represent the average value of triplicate samples. The error bars in Figure 1 are omitted in order to avoid visual clutter, but they are incorporated in the following figures which refer to the elements being studied separately.

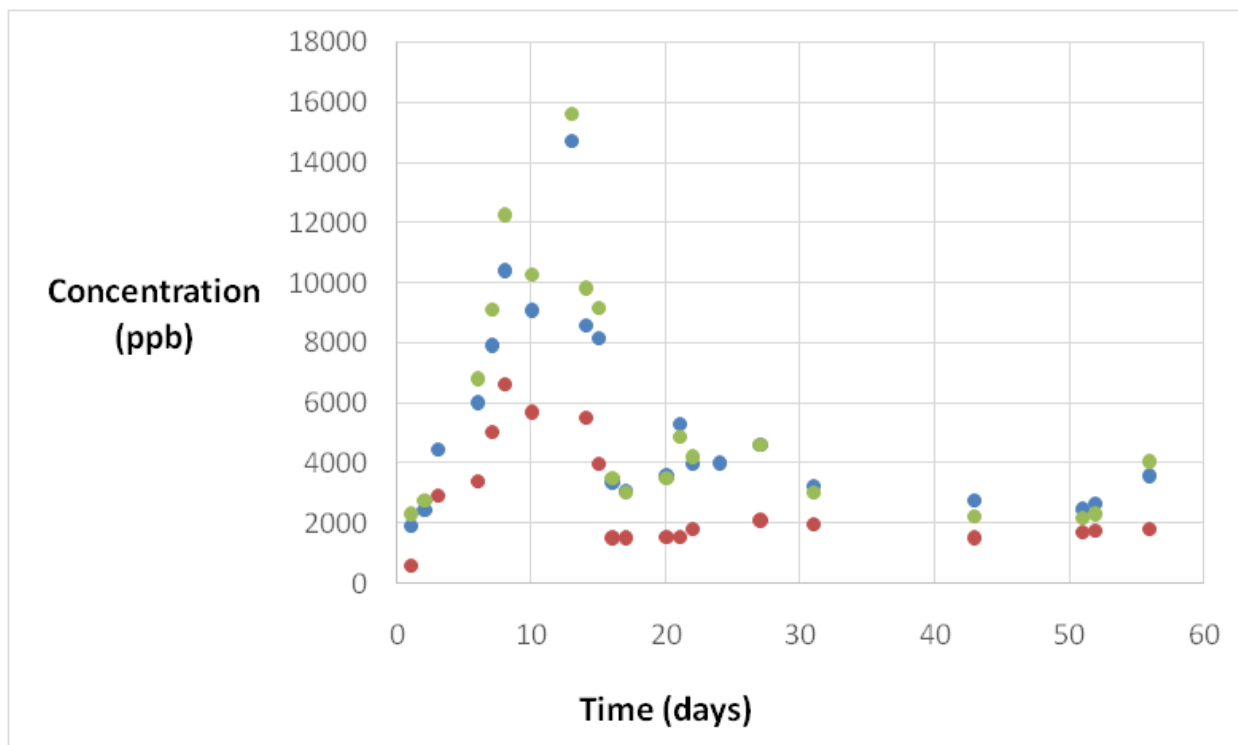


**Figure 1. Concentrations of Al (blue), Fe (red) and Si (green) released into the supernatant of batch experiments containing 4g of SRS F/H area soil (0.18<d<2 mm fraction) brought in contact with nitric acid solution of pH 2.5, as a function of time.**

Figure 1 reveals an identical pattern of release of Al, Fe and Si in the supernatant as a function of time due to contact with nitric acid. A gradual increase of the concentration is observed from the first day up to the eighth day and then a sharp decrease in the concentration takes place with a plateau observed beyond day 16.

For the time period 1-8 days, the concentrations of Al and Si were practically the same, taking into consideration that the two elements differ by only one atomic mass unit (Figure 2). Furthermore, the average rate of release was calculated for the two elements for this time period and was found to be  $3.5 \cdot 10^{-11} \pm 0.9 \cdot 10^{-11}$  mol/ml·min and  $3.8 \cdot 10^{-11} \pm 1 \cdot 10^{-11}$  mol/ml·min for Al and Si, respectively. All experiments were performed at room temperature (20° C). Quartz dissolution rate at pH 2.5 and 70° C is reported to be  $6.4 \cdot 10^{-14.3}$  mol/ml·min (Knaus and Wolery, 1987) and is expected to be magnitudes of order lower at room temperature. Hence, the preliminary results indicate that Al and Si release is taking place due to kaolinite dissolution with quartz dissolution having very little to no effect.

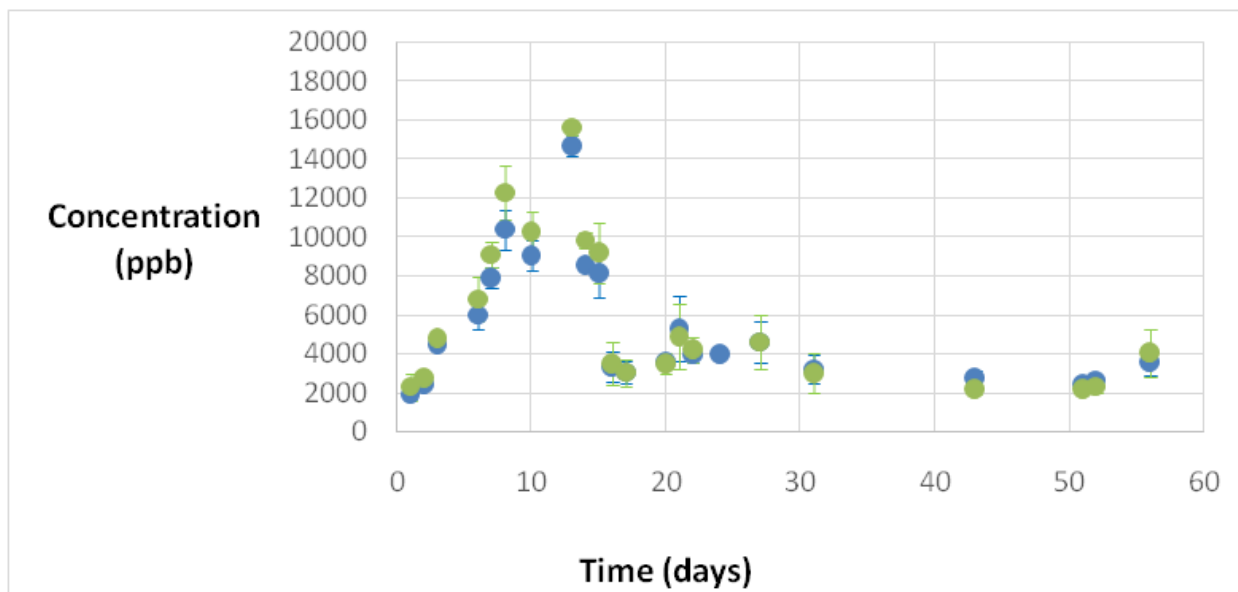


**Figure 2. Concentrations of Al (blue) and Si (green) released into the supernatant of batch experiments containing 4g of SRS F/H area soil (0.18<d<2 mm fraction) brought in contact with nitric acid solution of pH 2.5, as a function of time. Error bars represent the standard deviation of triplicate samples.**

Furthermore, there seems to be no preferential leaching of one element over the other. On the contrary, there seems to be a stoichiometric release of Al and Si in the supernatant, since these two elements are found in equimolar compositions at kaolinite's structure,  $\text{Al}_2\text{Si}_2\text{O}_5(\text{OH})_4$ . In literature, it has been reported that kaolinite dissolves congruently at 25° C for pH values lower than 4 and higher than 11, but incongruently in the in-between range (Carroll and Walther, 1990; Huertas et al., 1999). The set of data points for Day 13 is believed to be an outlier.

Iron follows a very similar pattern of release in the aqueous phase (Figure 3); nevertheless, the maximum amount of iron released (Day 8) is significantly lower than that of Al and Si: 6.6 ppm of Fe, as opposed to 12.2 ppm of Si and 10.4 ppm of Al. The average rate of Fe release was found to be  $7.2 \cdot 10^{-12} \pm 2 \cdot 10^{-12}$  mol/ml·min, which is significantly lower than the corresponding rates of Al and Si release. This result could be expected, since the concentration of Fe in the SRS soil (in the form of goethite) is lower than that of Al and Si, mostly present in the form of kaolinite and montmorillonite).



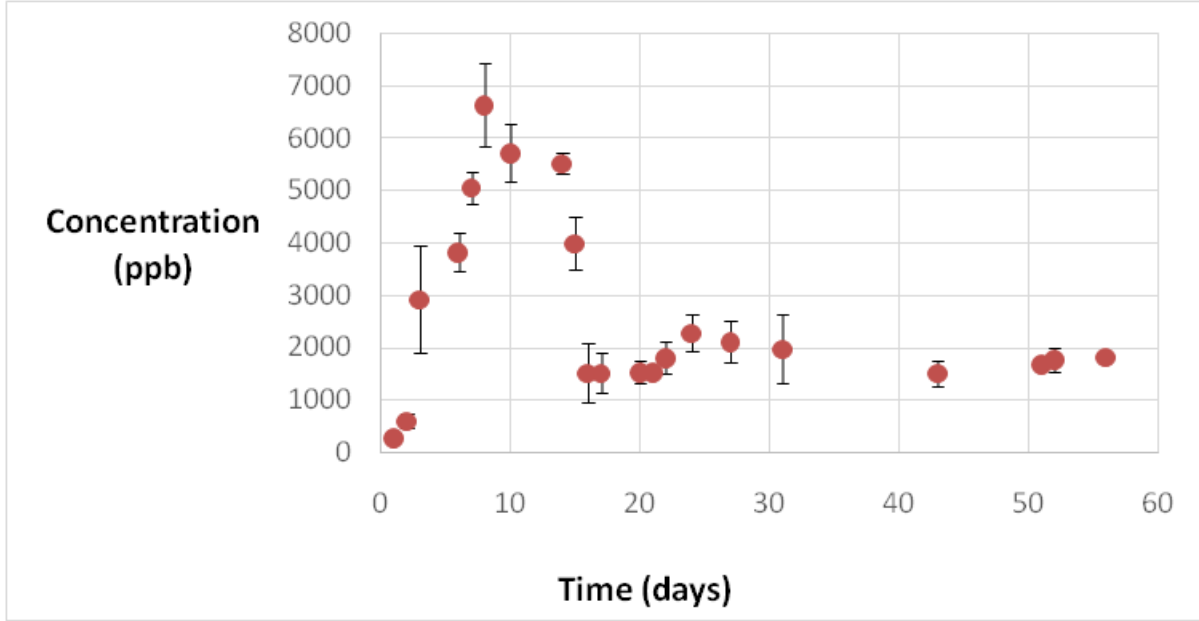


**Figure 3.** Concentrations of Fe released into the supernatant of batch experiments containing 4g of SRS F/H area soil (0.18<d<2 mm fraction) brought in contact with nitric acid solution of pH 2.5, as a function of time. Error bars represent the standard deviation of triplicate samples.

The elemental composition of the specific fraction was calculated in our previous experiments by means of SEM-EDS. In Table 1, the elemental composition is presented, along with the percentage of each element leached in the supernatant based on the maximum concentration determined (Day 8).

**Table 1.** Concentration of Fe, Al and Si for Each SRS Fraction Followed by Relative Standard Deviation and Percentage Leached During the Preliminary Kinetic Experiment

SRS Soil Fraction	[Fe]	[Al]	[Si]	Percentage leached		
	(mg/g)	(mg/g)	(mg/g)	Fe	Al	Si
180µm<d<2mm	40±4	54±13	416±37	0.5%	0.6%	0.1%

It should be noted that the release of Si is much lower, since the elemental analysis of Si in the soil by means of SEM-EDS provides the total mass of Si, which can be traced back to both quartz and kaolinite. Nevertheless, our preliminary kinetic results did not reveal quartz dissolution.

The gradual decrease in concentrations of the elements being studied and the creation of a plateau can be explained by speciation calculations. With the aid of Visual Minteq, a list of

aqueous species and saturated solids was created under the conditions studied and is presented in Table 2. Concentrations of Al, Fe and Si in the calculations were derived from Day 8 experimental points (“peaks”), with atmospheric CO<sub>2</sub> included as well.

**Table 2. Major Aqueous and Saturated Species at pH 2.5, as Predicted by Visual Minteq**

<b>Aqueous species</b>	<b>Saturated solids</b>
Al <sup>3+</sup>	Goethite - FeO(OH)
H <sub>4</sub> SiO <sub>4</sub>	Hematite – Fe <sub>2</sub> O <sub>3</sub>
Fe <sup>3+</sup>	Lepidocrocite – γ-FeO(OH)
Fe(OH) <sup>2+</sup>	Quartz & Chalcedony – SiO <sub>2</sub>

The software predicts the formation of several Fe- and Si-bearing solids, which are in equilibrium with the Fe and Si aqueous species (plateau). Nevertheless, under the conditions studied there were no aluminosilicates or other Al-bearing solids predicted, a fact that would explain the decrease in Al concentration. Kaolinite (Al<sub>2</sub>Si<sub>2</sub>O<sub>5</sub>(OH)<sub>4</sub>) and pyrophyllite (Al<sub>2</sub>Si<sub>4</sub>O<sub>10</sub>(OH)<sub>2</sub>) are either under saturation or their formation is not thermodynamically favored, based on speciation calculations by both software packages (Visual Minteq and Hydra-Medusa). In Figure 4 and Figure 5 the speciation diagrams made with the Hydra-Medusa chemical equilibrium diagram software are presented. An explanation of this phenomenon could be the co-precipitation of dissolved Al with the existing soil minerals and during the formation of iron- and silicon-bearing solids.

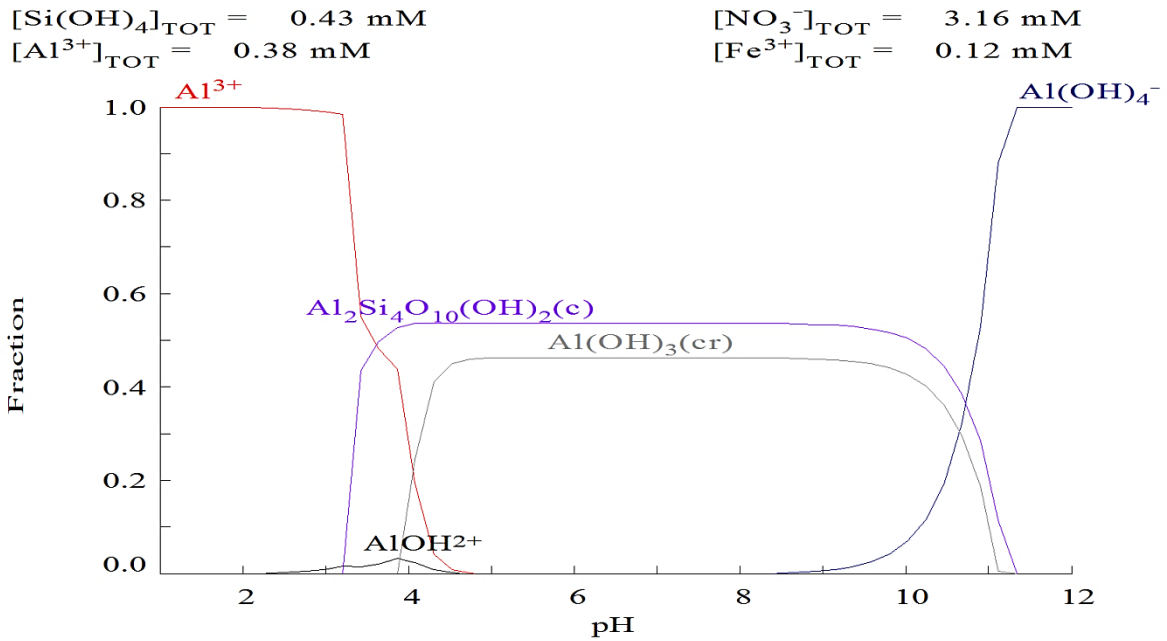


Figure 4. Speciation diagram of aqueous species and solid phases as a function of pH for Al, predicted by Hydra-Medusa Equilibrium Speciation Diagram.

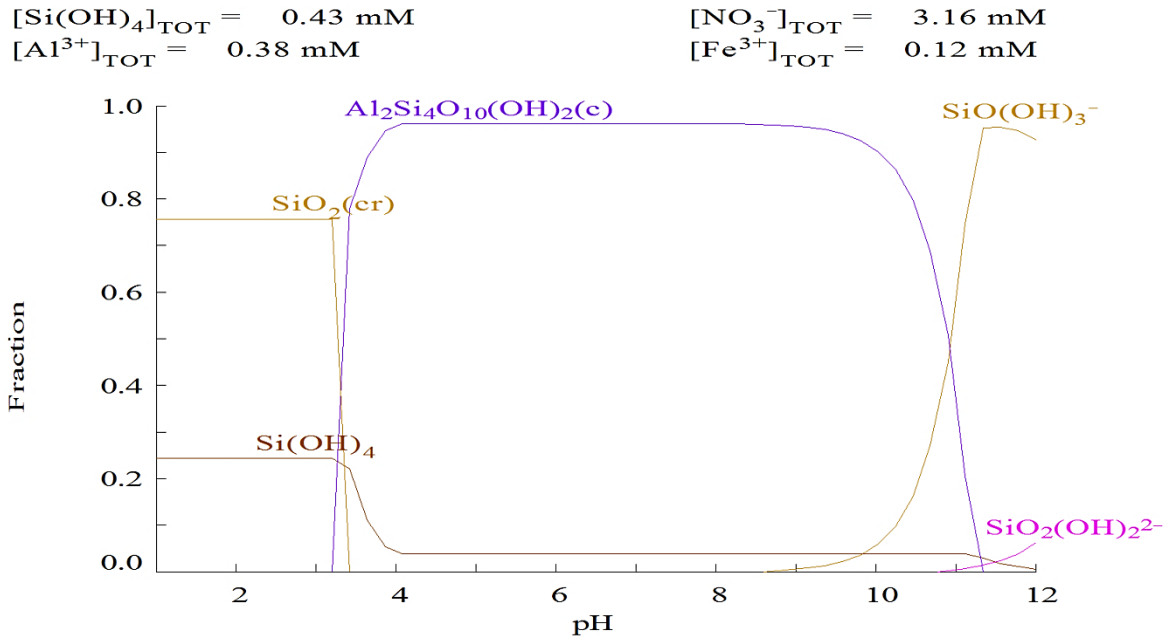
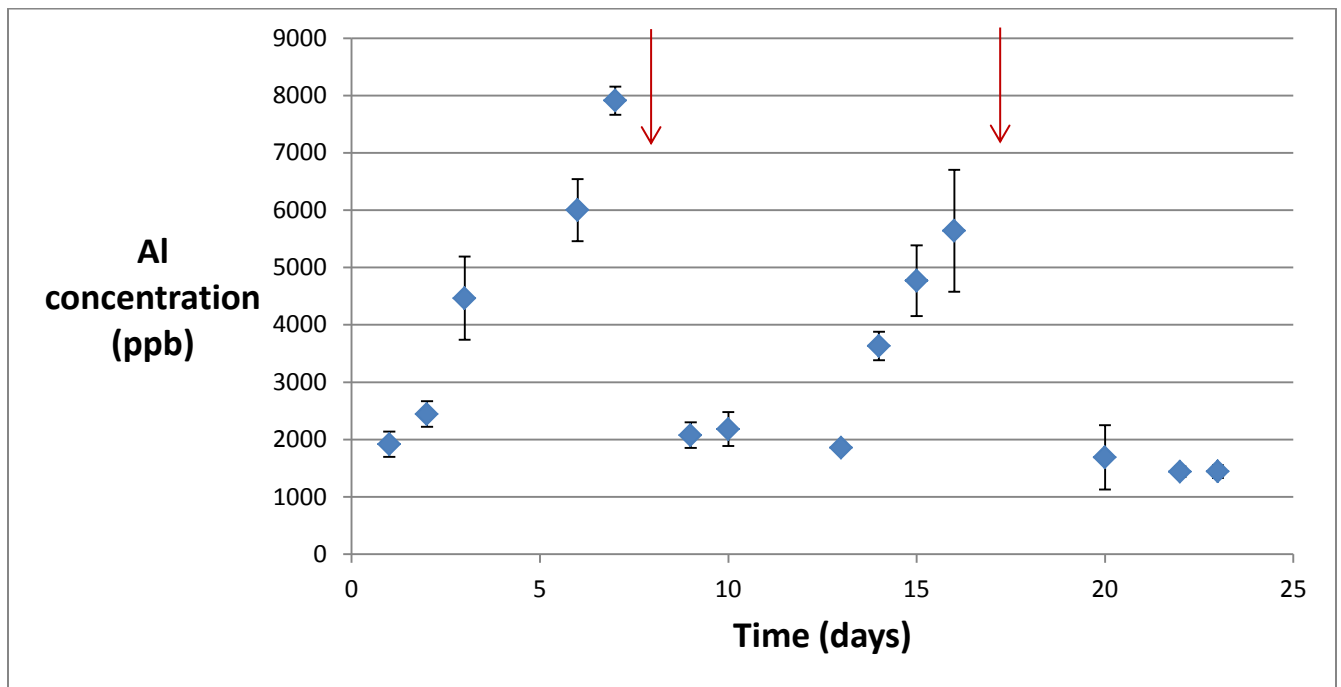


Figure 5. Speciation diagram of aqueous species and solid phases as a function of pH for Si, predicted by Hydra-Medusa Equilibrium Speciation Diagram.

#### 4.2 Creation of Different Profiles of Acid-Treated Soil

Based on the preliminary kinetic results, batch experiments were performed with the aqueous phase replenished every 7 days, and the concentrations of Fe, Al and Si were monitored. The purpose of this experiment (ongoing) is to obtain soil that has come in contact with nitric acid solution at pH 2.5 for different time intervals. This would help to identify changes on the soil physico-chemical properties due to this interaction affecting contaminant sorption.

The results are presented in Figure 6, Figure 7, Figure 8 and Figure 9.



**Figure 6. Concentration of Al (ppb) in the supernatant solution as a function of time. Error bars represent the standard deviation of triplicate samples. Red arrows are pointing to the time interval where the supernatant was replenished.**

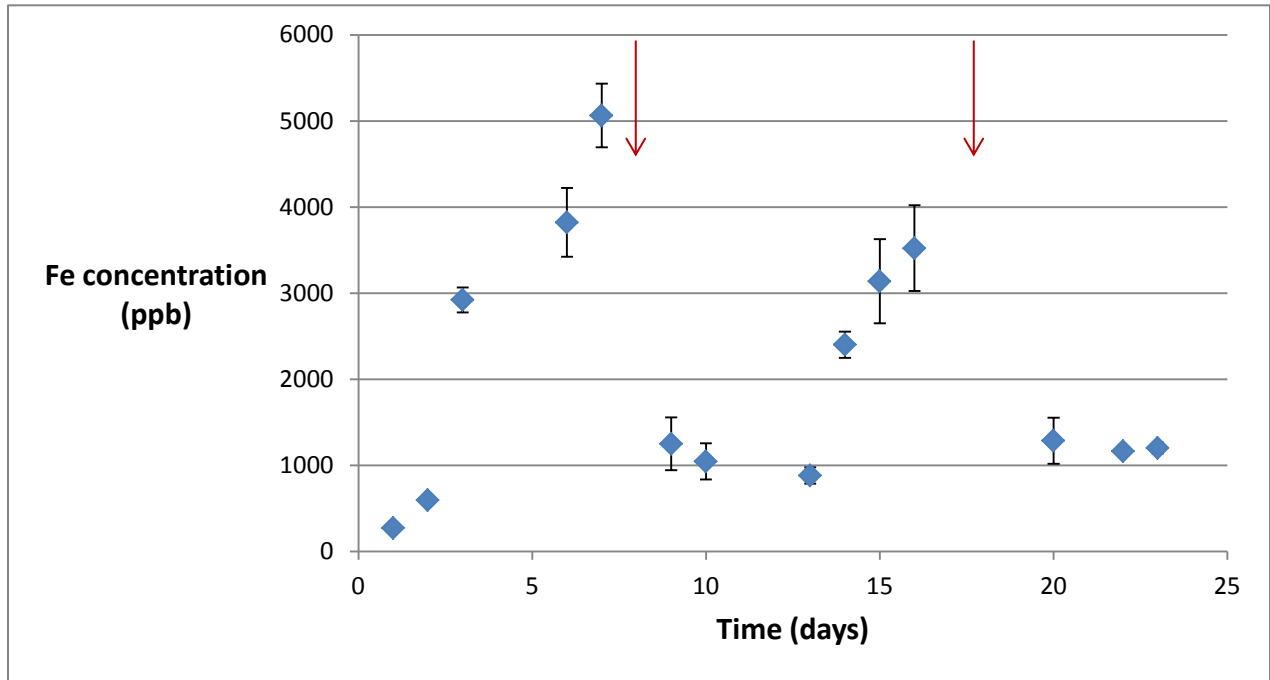


Figure 7. Concentration of Fe (ppb) in the supernatant solution as a function of time. Error bars represent the standard deviation of triplicate samples. Red arrows are pointing to the time interval where the supernatant was replenished.

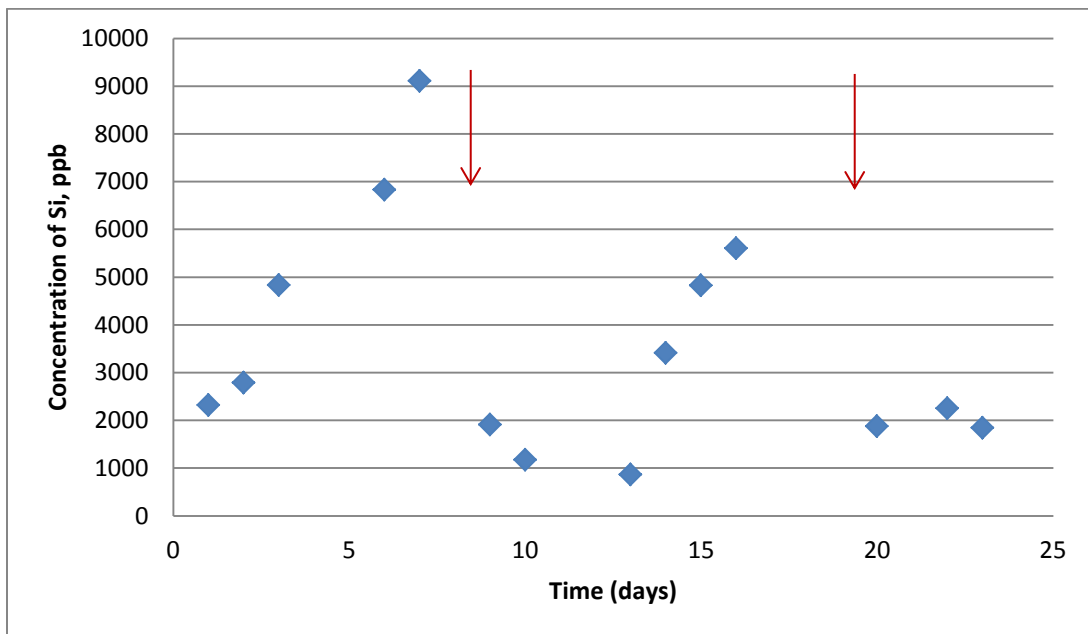
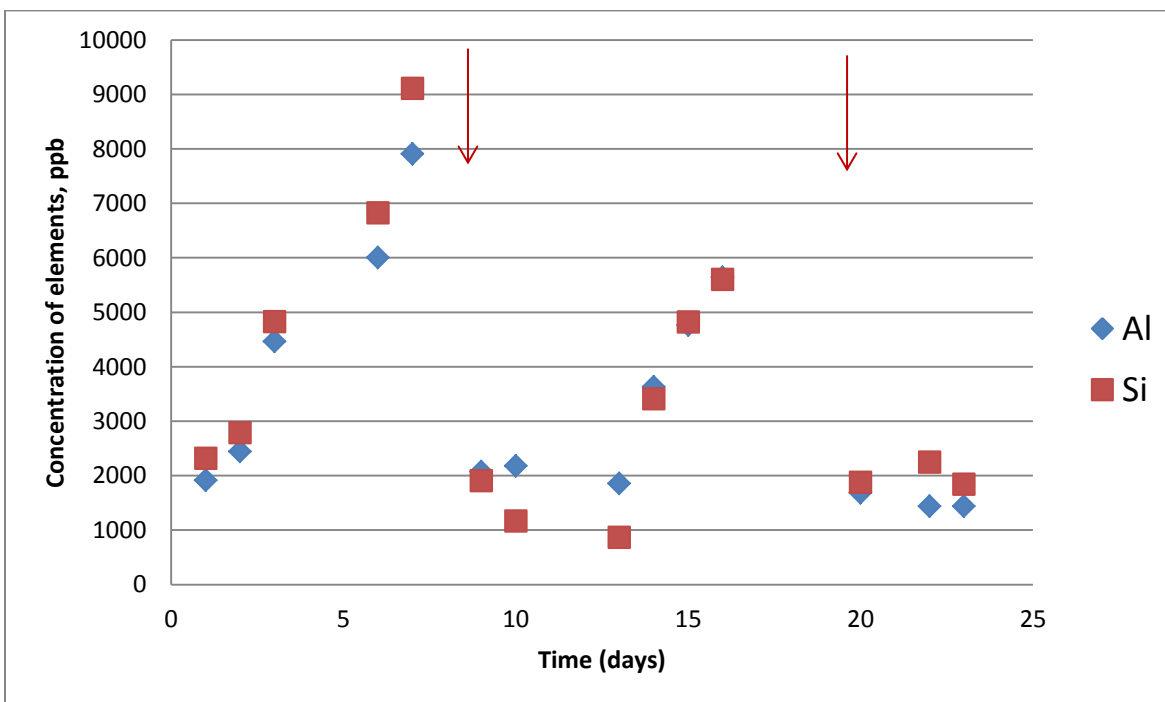


Figure 8. Concentration of Si (ppb) in the supernatant solution as a function of time. Error bars represent the standard deviation of triplicate samples. Red arrows are pointing to the time interval where the supernatant was replenished.

The elemental concentration gradually increases for all elements during the first 7 days and once the supernatant is replenished, the concentration drops to the initial levels. A lag period is observed for all three elements after each replenishment; the concentration of the elements remains stable for the first 3-4 days and then gradually increases. Furthermore, the maximum amount of each element released into the supernatant is significantly smaller than the corresponding amount during the first cycle. For example, the maximum concentration of Al during the first cycle was found to be 8 ppm, while for the second cycle it was 5.6 ppm; for Fe, it was 5 ppm during the first cycle versus 3.5 ppm during the second; and for Si, it was 9 ppm during the first cycle versus 5.6 ppm during the second. This pattern may be explained by the assumption that acid first “washes out” all fine particles present in the soil, which are more readily available due to their higher specific surface, and during the second and third cycle, larger particles are being more slowly dissolved. Finally, there seems to be no preferential dissolution of Al and Fe so far, since the concentrations are almost the same (Figure 9).



**Figure 9.** Concentration of Al and Si (ppb) in the supernatant solution as a function of time. Error bars represent the standard deviation of triplicate samples. Red arrows are pointing to the time interval where the supernatant was replenished.

## 5. Future Work

Future work will include the determination of the specific surface area and pore distribution of soil isolated at different time intervals and use the obtained acid treated soil samples for sorption experiments with U(VI). The results will be compared to the corresponding results of U(VI) on

SRS F Area background and contaminated soil. A triplicate has already been isolated at the end of the first cycle and another triplicate will be isolated at the end of the third cycle.

## 6. References

Carroll S.A., Walther J.V. (1990). Kaolinite dissolution at 25<sup>o</sup>, 60<sup>o</sup> and 80<sup>o</sup> C. *American Journal of Science* 290, 797-810.

Huertas J.H., Chou L., Wollast R. (1999) Mechanism of kaolinite dissolution at room temperature and pressure. Part II: kinetic study. *Cosmochimica et Geochimica Acta* 63, 3261-3275.

Knauss K.G., Wolery T.J. (1987). The dissolution kinetic of quartz as a function of pH and time at 70<sup>o</sup>C. *Cosmochimica et Geochimica Acta* 52, 43-53.